
A BAYESIAN APPROACH FOR FITTING SEMI-MARKOV MIXTURE MODELS OF CANCER LATENCY TO INDIVIDUAL-LEVEL DATA

A PREPRINT

 **Raphaël N. Morsomme**

Department of Statistical Science
Duke University
Durham, NC 27710

 **Shannon T. Holloway**

Department of Population Health Sciences
Duke University School of Medicine
Durham, NC 27710

 **Marc D. Ryser***

Department of Population Health Sciences
Department of Mathematics
Duke University
Durham, NC 27710
marc.ryser@duke.edu

 **Jason Xu***

Department of Statistical Science
Duke University
Durham, NC 27710
jason.q.xu@duke.edu

ABSTRACT

Multi-state models of cancer natural history are widely used for designing and evaluating cancer early detection strategies. Calibrating such models against longitudinal data from screened cohorts is challenging, especially when fitting non-Markovian mixture models against individual-level data. Here, we consider a family of semi-Markov mixture models of cancer natural history introduce an efficient data-augmented Markov chain Monte Carlo sampling algorithm for fitting these models to individual-level screening and cancer diagnosis histories. Our fully Bayesian approach supports rigorous uncertainty quantification and model selection through leave-one-out cross-validation, and it enables the estimation of screening-related overdiagnosis rates. We demonstrate the effectiveness of our approach using synthetic data, showing that the sampling algorithm efficiently explores the joint posterior distribution of model parameters and latent variables. Finally, we apply our method to data from the US Breast Cancer Surveillance Consortium and estimate the extent of breast cancer overdiagnosis associated with mammography screening. The sampler and model comparison method are available in the R package `baclava`.

*Joint senior authors

Keywords Cancer natural history · Cancer indolence · Overdiagnosis · Data augmentation · Markov chain Monte Carlo

1 Introduction

Cancer screening aims to detect early signs or markers of cancer before symptoms arise, facilitating timely intervention for improved patient outcomes. The efficacy of screening depends on the duration of the pre-clinical phase, during which the tumor is asymptomatic but screen-detectable. If the latency period of a tumor is too short, even frequent screening does not significantly advance the time of diagnosis. Conversely, a long latency period can result in *overdiagnosis*—the diagnosis and unnecessary treatment of slowly growing tumors that would not have caused symptoms or other harm in the person’s remaining lifetime [Welch and Black, 2010, Duffy and Parmar, 2013]. Understanding the duration of tumor latency is thus crucial for assessing the balance between the benefits and harms of a screening test.

Estimating tumor latency from cancer incidence data is challenging, because the onset of pre-clinical disease in healthy individuals is not directly observable. In unscreened populations, only the time of clinical diagnosis, which coincides with the end of the tumor latency period, is known. In this case, we cannot distinguish the time intervals before and after pre-clinical onset. In other words, the period of tumor latency is not identifiable. Fortunately, screening methods that utilize biological or imaging markers offer a selective insight into the latent disease state, thus enabling the identification of tumor latency.

There is a rich history on estimating cancer latency from screening data using multi-state models that dates back to the 1980s. These models range from simple three-state models [Day and Walter, 1984, Shen and Zelen, 1999]—in which individuals are *healthy* (disease-free), *pre-clinical* (with an asymptomatic screen-detectable cancer) or *clinical* (with a symptomatic cancer)—to more complex models that seek to emulate the biological complexity of cancer progression [Rutter and Savarino, 2010, Seigneurin et al., 2011]. Typically, the underlying stochastic processes of cancer natural history models are assumed to be Markovian for mathematical tractability. Under this assumption, the unobserved onset times can be integrated out analytically, giving a closed-form expression for the likelihood of observed data. This enables maximum likelihood estimation [Olsen et al., 2006, Wu et al., 2018] and Bayesian inference [Duffy et al., 2005, Ryser et al., 2022]. However, relaxing the Markov assumption of state transitions often leads to a departure from the simpler mathematical structures, and the calibration of more complex non-Markovian models is usually performed using simulation-based or “likelihood-free” approximation methods, such as approximate Bayesian computation [Rutter et al., 2009, Alagoz et al., 2018, Bondi et al., 2023] or pseudo-likelihood methods [Moore et al., 2001].

In this paper, we present a method for exact Bayesian inference of cancer natural history using a flexible family of semi-Markov mixture models that account for both progressive and non-progressive (indolent) disease states. The proposed approach accommodates individual-level screening and cancer diagnosis histories, and, because it does not rely on model-based simulation, is scalable to large cohorts of screened individuals. By relaxing the Markov assumption, we may then flexibly specify the hazard function, which in turn leads to improved model realism [Hsieh et al., 2002, Cheung et al., 2022]. Since the semi-Markov models do not admit a closed form expression for the observed data likelihood, we conduct inference using data augmentation [Tanner and Wong, 1987]. This strategy augments the

observed data with latent variables in such a way that the resulting *complete-data* likelihood is amenable to iterative sampling. Executing this idea in the context of cancer natural history modeling is nontrivial because there are twice as many latent variables as the number of individuals in the study, and cancer screening cohorts often comprise tens or hundreds of thousands of individuals. The resulting joint posterior distribution is complex and high-dimensional, rendering standard rejection or importance sampling approaches impractical. Moreover, gradient-based approaches, such as Hamiltonian Monte Carlo, which are well-suited for high-dimensional problems [Girolami and Calderhead, 2011], are not applicable to our family of models due to the presence of discrete latent variables, and of discontinuities in the likelihood from the discrete screening outcomes.

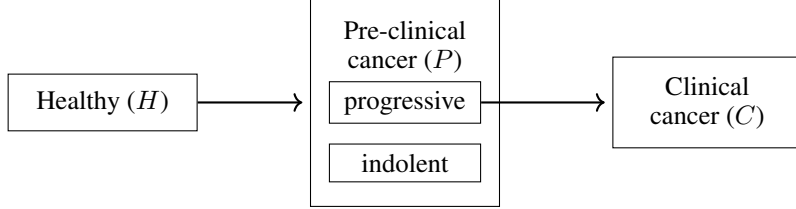
Instead, our data-augmented Markov chain Monte Carlo (DA-MCMC) sampler efficiently explores the joint posterior distribution of the model parameters together with the latent variables, enjoying sound theoretical guarantees. This fully Bayesian approach automatically accounts for the uncertainty in the exact onset time of pre-clinical cancers, and allows the estimation of any relevant function of the parameters such as the overdiagnosis rate through their posterior distribution. In addition, because the complete-data likelihood has a simple closed form, we can rigorously compare and select models using an extension of approximate leave-one-out cross-validation [Gelfand et al., 1992, Gelfand, 1995, Vehtari et al., 2017] to latent data models.

The paper is structured as follows. In Section 2, we introduce the underlying family of semi-Markov mixture models of cancer natural history; in Section 3, we describe the inferential framework; and, in Section 4, we detail the construction of the DA-MCMC algorithm. We examine the mixing properties of the sampler through simulation studies in Section 5 and apply it to estimate the extent of overdiagnosis in a real-world cohort of women undergoing mammography screening in Section 6. The DA-MCMC sampling algorithm is publicly available in the R package `baclava`, and R code for reproducing the results present in this paper is available on GitHub (<https://github.com/rmorsomme/baclava-manuscript>).

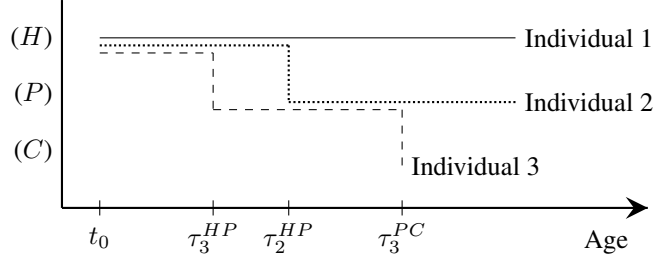
2 Semi-Markov mixture model of cancer progression

We model the dynamics of cancer progression as a multi-state mixture model. The model, depicted in Figure 1a, consists of the three compartments *healthy* (H), *pre-clinical cancer* (P) and *clinical cancer* (C). Following Ryser et al. [2019], pre-clinical cancers are modeled as a mixture of progressive and indolent tumors. All individuals start in the healthy state H , and transition to a state of pre-clinical screen-detectable cancer P after a randomly distributed time. Once in P , individuals with an indolent cancer stay in this compartment indefinitely, while individuals with a progressive cancer eventually transition to C when their cancer becomes symptomatic.

Several early works consider purely progressive models, in which all pre-clinical tumors progress to clinical disease after a finite time [Day and Walter, 1984, Shen and Zelen, 1999, 2001]. Allowing a proportion of pre-clinical cancers to be non-progressive is particularly important for slowly growing or indolent disease entities, such as low-risk prostate cancers or *in situ* breast cancers [Baker et al., 2014]. Despite the challenges of fitting such mixture models in practice [Ryser et al., 2019], these models have gained in popularity, especially in the study of breast cancer progression [Chen



(a) Compartmental model for cancer progression with a mixture of progressive and indolent pre-clinical cancers.



(b) Illustration of possible individual clinical trajectories through the compartmental model.

Figure 1: Panel (a) depicts the compartmental model for the progression of cancer. Panel (b) illustrates possible individual trajectories through the compartmental model. Individuals start in compartment H . Only transitions from H to P and from P to C are possible, with compartment P being an absorbing state for indolent individuals and compartment C being absorbing for all others. In Panel (b), individual 1 does not develop pre-clinical cancer before the end of the observation period and, therefore, remains in H until that time. Individual 2 develops pre-clinical cancer at age τ_2^{HP} , at which time they transition to P , but they do not develop clinical cancer before the end of the observation period and, therefore, remain in P . Note that the pre-clinical cancer of individual 2 may be either indolent, in which case $\tau_2^{PC} = \infty$, or progressive with a clinical onset time after the end of the observation period. Individual 3 develops pre-clinical cancer at age τ_3^{HP} and transitions to state P . At age τ_3^{PC} , they develop clinical cancer and thus transition to C . As C is absorbing, the observation period ends with their transition time into C .

et al., 1996, Duffy et al., 2005, Olsen et al., 2006, Seigneurin et al., 2011, Alagoz et al., 2018, Wu et al., 2018, Ryser et al., 2022].

To formalize the model structure, we let the starting age $t_0 \geq 0$ correspond to the age at which individuals become susceptible to developing pre-clinical cancer, so that the hazard rate of pre-clinical cancer is assumed to be zero before t_0 . Next, let τ^{HP} be the age at pre-clinical onset (the transition from H to P) and let τ^{PC} be the age at clinical onset (the transition from P to C); by definition, $t_0 \leq \tau^{HP} \leq \tau^{PC}$. When a tumor is indolent, we set $\tau^{PC} = \infty$, reflecting the fact that indolent cancers never progress to the clinical stage. Figure 1b illustrates the evolution of three individuals throughout this multi-state model.

The associated stochastic process is characterized by the probabilistic mechanisms governing the transitions between the compartments. Denote the waiting time until pre-clinical cancer with $\sigma^H = \tau^{HP} - t_0$ and the pre-clinical sojourn time with $\sigma^P = \tau^{PC} - \tau^{HP}$, corresponding to the interval between the onset of pre-clinical cancer and the diagnosis with symptomatic disease. An individual with an indolent tumor has $\sigma^P = \infty$. We assume that

$$\sigma^H \sim F_H, \quad \sigma^P \sim F_P, \quad (1)$$

independently, where F_H is a distribution on the positive line, and F_P corresponds to the mixture cure model [Berkson and Gage, 1952, Peng and Taylor, 2014],

$$F_P = \psi \delta_\infty + (1 - \psi) F_{\text{prog}}. \quad (2)$$

with a point mass at ∞ for indolent cancers and a density on the positive line for progressive cancers. Here, $\psi \in [0, 1]$ is the proportion of indolent cancers and δ_∞ the Dirac distribution with point mass at ∞ . Distribution (2) implies that a proportion ψ of tumors are indolent with infinite sojourn times while the sojourn time of progressive tumors follows distribution F_{prog} .

Our inferential framework will apply to arbitrary choices of parametric distributions on the positive line for F_H and F_{prog} , resulting in a flexible semi-Markovian formulation. We write θ to refer to the collective parameters of F_H and F_{prog} . This formulation encompasses existing models as special cases: for example, letting F_H and F_{prog} be exponential distributions results in the Markov mixture model of Seigneurin et al. [2011], and $\psi = 0$ recovers the purely progressive model of Shen and Zelen [1999, 2001]. Introducing the indolence indicator I , which equals 1 if the cancer is indolent and 0 otherwise, we can also express the distribution (2) hierarchically as

$$I \sim \text{Ber}(\psi), \quad (3)$$

$$\sigma^P \mid I \sim \begin{cases} \delta_\infty, & I = 1 \\ F_{\text{prog}}, & I = 0 \end{cases}, \quad (4)$$

where $\text{Ber}(p)$ denotes the Bernoulli distribution with probability parameter p .

3 Likelihood and inferential methodology

3.1 Likelihood of complete data

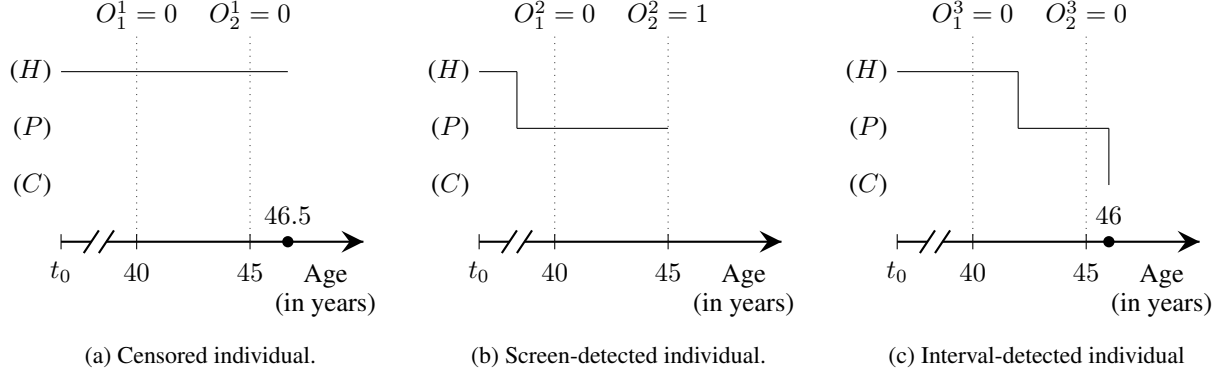
Consider a sample of n individuals that evolve independently, and let the subscript $i = 1, \dots, n$ refer to quantities related to the i th individual. We refer to the data for individual i as $X_i = (I_i, \tau_i^{HP}, \tau_i^{PC})$ and write $\mathbf{X} = (X_1, \dots, X_n)$ for the data of the entire population. By independence between the individuals, the likelihood of the process described by equations (1)-(4) factorizes as

$$\tilde{L}(\theta, \psi; \mathbf{X}) = \prod_{i=1}^n \tilde{L}_i(\theta, \psi; X_i) \quad (5)$$

where

$$\tilde{L}_i(\theta, \psi; X_i) = \begin{cases} S_H(c_i - t_0; \theta), & c_i < \tau_i^{HP} \\ f_H(\sigma_i^H; \theta) f_I(I_i; \psi) S_{\text{prog}}(c_i - \tau_i^{HP}; \theta)^{1-I_i}, & \tau_i^{HP} \leq c_i < \tau_i^{PC} \\ f_H(\sigma_i^H; \theta) (1 - \psi) f_{\text{prog}}(\sigma_i^P; \theta), & \tau_i^{PC} \leq c_i \end{cases}. \quad (6)$$

is the likelihood of person i observed until their censoring age c_i . Here, f . and S . are the density and survival function of the corresponding distribution F . and f_I is the probability mass function of the Bernoulli distribution (3).



(d) Observed screen data for the 3 individuals corresponding to Figures 2a-2c.

(e) Observed right-censored transition age into C , t_i^{PC} , and censoring age for the 3 individuals corresponding to Figures 2a-2c.

Figure 2: Observed data for the individuals depicted in Figure 1b. Panels (a-c): diagram displaying the trajectories and screen results. Panel (d): screen results. Panel (e): right-censored onset age of clinical cancer. In Panel (a), the individual does not develop pre-clinical cancer before their censoring age. They are in H at the two screen times, the two screens are therefore negative. They are censored at age 46.5, 1.5 years after their last screen. In Panel (b), the individual develops a pre-clinical before age 40. They are in P when the two screens take place. The first screen is a false negative, and the second is positive. They are censored at age 45, their age at the positive screen. In Panel (c), the individual develops a pre-clinical cancer between the first and second screen and a clinical cancer at 46. Their screen at age 45 is a false negative. The onset time of their clinical cancer at age 46 is observed.

We can understand the individual likelihood (6) as follows. The contribution of a person i to the likelihood $\tilde{L}(\theta; \mathbf{X})$ depends on which compartment they are in at age c_i . If individual i does not develop pre-clinical cancer by the censoring age ($c_i < \tau_i^{HP}$), then their contribution is the survival function $S_H(c_i - t_0; \theta)$ of F_H . If they develop pre-clinical cancer but not clinical cancer by the censoring time ($\tau_i^{HP} \leq c_i < \tau_i^{PC}$), then their contribution consists of the product of the density $f_H(\sigma_i^H; \theta)$ of F_H , the Bernoulli probability mass function of the indolence indicator $f_{\mathbb{I}}(I_i; \psi)$, and $S_{\text{prog}}(c_i - \tau_i^{HP}; \theta)^{1-I_i}$ which is either the constant function 1 for indolent cases ($I_i = 1$) or the survival function of F_{prog} for progressive cases ($I_i = 0$). Finally, if the individual develops clinical cancer by the censoring time ($\tau_i^{PC} \leq c_i$), then their contribution is the product of $f_H(\sigma_i^H; \theta)$, the probability $1 - \psi$ of a progressive cancer, and the density $f_{\text{prog}}(\sigma_i^P; \theta)$ of distribution F_{prog} .

3.2 Partially observed data

We now turn our attention to real-world data sources, such as prospective screening trials and observational screening cohorts. In such settings, the data consist of a series of screens and associated results, as well as clinical cancer diagnoses. Let n_i denote the number of screens available for person i , with their age and outcome at each of these screening times contained in the vectors $(t_1^i, \dots, t_{n_i}^i)$ and $(O_1^i, \dots, O_{n_i}^i) \in \{0, 1\}^{n_i}$, respectively, where $t_1^i = e_i$ corresponds to the age

at study entry. These data are complemented by the time $t_i^{PC} = \min \{c_i, \tau_i^{PC}\}$, which corresponds to either the age of diagnosis with a screen-detected cancer, the age of diagnosis with a clinical cancer, or to the age of censoring otherwise.

We assume that the screening ages are non-informative, that is, that they are *ignorable* or independent of the disease process and of the model parameters. Under this assumption, we may condition on them in our analysis [Gelman et al., 2013]. We therefore denote the observed variables of individual i with $Y_i = (O_1^i, \dots, O_{n_i}^i, t_i^{PC})$ and condition on the ignorable screen ages $(t_1^i, \dots, t_{n_i}^i)$. We further write $\mathbf{Y} = (Y_1, \dots, Y_n)$. Tables 2d and 2e present the observed data of a sample of three individuals for illustration.

The screening outcomes are modeled as mutually independent Bernoulli random variables

$$O_j^i \sim \text{Ber}(p_j^i), \quad j = 1, \dots, n_i, \quad i = 1, \dots, n, \quad \text{where} \quad p_j^i = \begin{cases} 0, & t_j^i < \tau_i^{HP} \\ \beta, & \tau_i^{HP} \leq t_j^i < \tau_i^{PC} \end{cases}. \quad (7)$$

Equation (7) indicates that the probability of positive screen p_j^i is 0 when a person is in the H compartment, while it becomes β when they are in P ; we see the parameter $\beta \in [0, 1]$ is interpreted as the *screening sensitivity* and is not assumed to be known. Upon a cancer diagnosis—whether clinical or screen-detected—an individual receives treatment and leaves the screening program, implying that any positive screen is the last screen of the individual. Consequently, p_j^i need not be defined when $t_j^i > \tau_i^{PC}$.

The observed data partition the individuals into three groups. The *censored* group consists of individuals with no positive screens and who do not develop a clinical cancer before their censoring age. These individuals either remain in H until their censoring age, or transition into P and remain there until their censoring age; any screens conducted when they are in P are false negatives (see Figure 2a). The *screen-detected* group includes individuals who are in state P at the time of the positive screen (see Figure 2b). Finally, the *interval-detected* group contains those with no positive screen but whose cancer reaches the clinical stage before their censoring age (see Figure 2c). These individuals may or may not have false negative screens.

3.3 Bayesian inference via data-augmented Markov chain Monte Carlo

We now describe how to conduct Bayesian inference to fit the semi-Markov model defined by Equations (1)-(4) to censored data \mathbf{Y} . By Bayes Theorem, $\pi(\theta, \psi, \beta \mid \mathbf{Y}) \propto \pi(\theta, \psi, \beta)L(\theta, \psi, \beta; \mathbf{Y})$ where $\pi(\theta, \psi, \beta)$ is the prior distribution of the parameters θ, ψ and β , and the marginal likelihood

$$L(\theta, \psi, \beta; \mathbf{Y}) = \int f(\mathbf{Y} \mid \mathbf{x}, \theta, \psi, \beta)L(\theta, \psi; \mathbf{x})d\mathbf{x}, \quad (8)$$

is related to the complete-data likelihood (5) via integration. Equation (8) integrates over all the possible clinical histories of the individuals consistent with the observed data. No general closed-form expression for this integral exists in the semi-Markov case [Hsieh et al., 2002], and numerical integration over this high-dimensional latent space is intractable.

To overcome this difficult integration step, data-augmented MCMC takes advantage of the tractable form (5). The observed data \mathbf{Y} are augmented with the latent variables \mathbf{Z} such that $L(\theta, \psi; \mathbf{Z})$ and $f(\mathbf{Y} \mid \theta, \psi, \beta, \mathbf{Z})$ have closed-form expressions. We can then use Markov chain Monte Carlo to sample from the joint posterior distribution

$$\pi(\theta, \psi, \beta, \mathbf{Z} \mid \mathbf{Y}) \propto f(\mathbf{Y} \mid \theta, \psi, \beta, \mathbf{Z})L(\theta, \psi; \mathbf{Z})\pi(\theta, \psi, \beta). \quad (9)$$

Given M MCMC draws $\{(\theta^{(m)}, \psi^{(m)}, \beta^{(m)}, \mathbf{Z}^{(m)})\}_{m=1}^M$, marginalizing out latent variables *a posteriori* becomes trivial. The values $\{(\theta^{(m)}, \psi^{(m)}, \beta^{(m)})\}_{m=1}^M$ form an empirical approximation to the original distribution of interest $\pi(\theta, \psi, \beta \mid \mathbf{Y})$. In other words, simply ignoring the latent variables in each posterior sample yields a valid marginal posterior of the parameters of interest. Similarly, $\{\mathbf{Z}^{(m)}\}_{m=1}^M$ form a Monte Carlo approximation to $\pi(\mathbf{Z} \mid \mathbf{Y})$.

An advantage of the Bayesian formulation is that inference is not limited to θ, ψ, β and \mathbf{Z} . The posterior distribution $\pi(g(\cdot) \mid \mathbf{Y})$ of any functional $g(\theta, \psi, \beta, \mathbf{Z})$ is approximated by the transformed sample $\{g^{(m)}\}_{m=1}^M$, with $g^{(m)} = g(\theta^{(m)}, \psi^{(m)}, \beta^{(m)}, \mathbf{Z}^{(m)})$. In Section 6, we will be interested in g being the overdiagnosis rate.

In our model, the latent variables \mathbf{Z} consist of the unknown transition ages into P and the indolent status of each individual. We write $\mathbf{Z} = (\mathbf{Z}_1, \dots, \mathbf{Z}_n)$, where $\mathbf{Z}_i = (Z_i^{HP}, Z_i^I)$ are the latent variables of individual i . $Z_i^{HP} \in (t_0, c_i] \cup \emptyset$ denotes the pre-clinical onset age and $Z_i^I \in \{0, 1\}$ the indolent status. Here, \emptyset indicates the event that the corresponding transition age is larger than c_i .

Upon introducing these latent variables, we have closed-form expressions for $L(\theta, \psi; \mathbf{Z})$ and $f(\mathbf{Y} \mid \theta, \psi, \beta, \mathbf{Z})$. First, by independence, we have

$$L(\theta, \psi; \mathbf{Z}) = \prod_{i=1}^n L_i(\theta, \psi; \mathbf{Z}_i) = \prod_{i=1}^n \tilde{L}_i(\theta, \psi; \mathbf{Z}_i) / N_i(\theta, \psi, e_i), \quad (10)$$

where

$$\tilde{L}_i(\theta, \psi; \mathbf{Z}_i) \propto f(\mathbf{Z}_i \mid \theta, \psi) = \begin{cases} S_{\mathbb{H}}(c_i - t_0; \theta), & Z_i^{HP} = \emptyset, \\ f_{\mathbb{H}}(Z_i^{HP} - t_0; \theta) f_{\mathbb{I}}(Z_i^I; \psi), & Z_i^{HP} \leq c_i \end{cases}, \quad (11)$$

and

$$\begin{aligned} N_i(\theta, \psi, e_i) &= \Pr(\tau_i^{PC} > e_i \mid \theta, \psi) \\ &= \Pr(I_i = 1) + \Pr(I_i = 0, \tau_i^{HP} > e_i) + \Pr(I_i = 0, \tau_i^{HP} < e_i < \tau_i^{PC}) \\ &= \Pr(I_i = 1) + \Pr(I_i = 0) [\Pr(\tau_i^{HP} > e_i \mid I_i = 0) + \Pr(\tau_i^{HP} < e_i, e_i < \tau_i^{PC} \mid I_i = 0)] \\ &= \psi + (1 - \psi) \left[S_{\mathbb{H}}(e_i - t_0; \theta) + \int_{t_0}^{e_i} f_{\mathbb{H}}(t - t_0; \theta) S_{\text{prog}}(e_i - t; \theta) dt \right]. \end{aligned} \quad (12)$$

scale the contribution from person i by the probability that they did not develop clinical cancer before entering the study at age e_i . The inclusion of the factor (12) in the likelihood (10) comes from the fact that data from cohort analyses are left-truncated: study participants that developed clinical cancer before the study are excluded. Therefore, we condition on the fact that the individuals in the sample have not developed clinical cancer before entering the study. As long as

f_H and S_{prog} are continuous and bounded, the univariate integral in (12) is easy to approximate numerically using a quadrature rule (e.g., the function `integrate` in base R).

Second, by independence, we have

$$f(\mathbf{Y} \mid \theta, \psi, \beta, \mathbf{Z}) = \prod_{i=1}^n f(Y_i \mid \mathbf{Z}_i, \theta, \psi, \beta), \quad (13)$$

where

$$f(Y_i \mid \mathbf{Z}_i, \theta, \psi, \beta) = f_t(t_i^{PC} \mid \mathbf{Z}_i, \theta) f_O(O_1^i, \dots, O_{n_i}^i \mid \mathbf{Z}_i, \beta); \quad (14)$$

the distribution of the right-censored clinical onset age is

$$f_t(t_i^{PC} \mid \mathbf{Z}_i, \theta) = \begin{cases} \delta_{c_i}(t_i^{PC}), & Z_i^{HP} = \emptyset, \\ S_{\text{prog}}(c_i - Z_i^{HP}; \theta)^{1-Z_i^I} \delta_{c_i}(t_i^{PC}) + f_{\text{prog}}(t_i^{PC} - Z_i^{HP}; \theta) \delta_{\tau_i^{PC}}(t_i^{PC}), & Z_i^{HP} \leq c_i \end{cases}, \quad (15)$$

and the distribution of the screen outcomes is

$$f_O(O_1^i, \dots, O_{n_i}^i \mid \mathbf{Z}_i, \beta) = \prod_{j=1}^{n_i} (p_j^i)^{O_j^i} (1 - p_j^i)^{1-O_j^i} = \beta^{m_i^+} (1 - \beta)^{m_i^-}, \quad (16)$$

where $m_i^+ = \sum_{j=1}^{n_i} O_j^i$ denotes the number positive screens of person i , and $m_i^- = \sum_{j: Z_i^{HP} \leq t_j^i} (1 - O_j^i)$ their number of false negative screens.

3.3.1 Prior specification

While the sampling methodology applies to any prior formulation $\pi(\theta, \psi, \beta)$, we assume for convenience here that the parameters are independent *a priori*

$$\pi(\theta, \psi, \beta) = \pi(\theta)\pi(\psi)\pi(\beta), \quad (17)$$

Moreover, we specify the prior distribution of β to be $\pi(\beta) = \text{Be}(a_\beta, b_\beta)$ and that of ψ to be $\pi(\psi) = \text{Be}(a_\psi, b_\psi)$, where $\text{Be}(a, b)$ denotes to the beta distribution with density proportional to $x^{a-1}(1-x)^{b-1}$. The choice of a beta prior distribution for β is motivated by conjugacy. Theorem 1 holds for any choice of F_H and F_{prog} .

Theorem 1 (Conjugacy). *If β is independent of the other parameters *a priori*, then the beta distribution is conjugate to the conditional likelihood in (9) for β . In particular, under the prior distribution*

$$\pi(\theta, \psi, \beta) = \pi(\theta)\pi(\psi)\pi(\beta), \quad \pi(\beta) = \text{Be}(a, b), \quad (18)$$

the full conditional distribution of β is

$$\pi(\beta \mid \theta, \psi, \mathbf{Z}, \mathbf{Y}) = \text{Be}(a + m^+, b + m^-), \quad (19)$$

with $m^+ = \sum_{i=1}^n m_i^+$ and $m^- = \sum_{i=1}^n m_i^-$ the total number of true positive and false negative screens in the sample, respectively.

Proof. The complete proof appears in Appendix A. \square

4 Markov chain Monte Carlo scheme

We propose a data-augmented Markov chain Monte Carlo sampler that alternates between a Gibbs update for β , Metropolis-Hastings steps for the elements of θ , and for $Z_1^{HP}, \dots, Z_n^{HP}$, and a block Metropolis-Hastings update of $(\psi, Z_1^I, \dots, Z_n^I)$. Updating ψ and (Z_1^I, \dots, Z_n^I) jointly is advantageous because we find these quantities are highly correlated *a posteriori*. This sampling scheme is summarized as a pseudo-algorithm in Algorithm 1. We note that methodologically, the elements of θ could also be jointly updated in a block Metropolis-Hastings step which may lead to further efficiency gains, though we do not explore this here.

Algorithm 1 Data-augmented Markov chain Monte Carlo

Require: a number of iterations M , initial values $(\theta^{(0)}, \psi^{(0)}, \beta^{(0)})$, and observed data \mathbf{Y}

$\mathbf{Z}^{(0)} \leftarrow \text{initialize } (\theta^{(0)}, \psi^{(0)}, \beta^{(0)})$

for $m = 1, \dots, M$ **do**

$\beta^{(m)} \sim \pi(\beta | \cdot)$ [Gibbs update, c.f. Theorem 1]

for $j = 1, \dots, |\theta|$ **do**

$\theta_j^{(m)} \leftarrow \text{Metropolis-Hastings}(\theta_j; \cdot)$ [update the j th element of θ]

end for

for $i = 1, \dots, n$ **do**

$(Z_i^{HP})^{(m)} \leftarrow \text{Metropolis-Hastings}(Z_i^{HP}; \cdot)$

end for

$\psi^{(m)}, (Z_1^I, \dots, Z_n^I)^{(m)} \leftarrow \text{Metropolis-Hastings}(\psi, Z_1^I, \dots, Z_n^I; \cdot)$

end for

return $\{(\theta^{(m)}, \psi^{(m)}, \beta^{(m)}, \mathbf{Z}^{(m)})\}_{m=1}^M$

Next, we briefly review Gibbs and Metropolis-Hastings updates [Brooks et al., 2011]. The Gibbs step for β proceeds by drawing a new value for this parameter from its full conditional distribution (19) given the most recent values of \mathbf{Z} . For the Metropolis-Hastings steps, consider the random vector (ζ, η) where ζ and η are random vectors and from which we wish to update ζ . Given current values $(\tilde{\zeta}, \tilde{\eta})$, a candidate value ζ^* is drawn according to the proposal density $q(\zeta^* | \tilde{\zeta}, \tilde{\eta})$, and is accepted with probability

$$\alpha(\tilde{\zeta}, \tilde{\eta} \rightarrow \zeta^*, \tilde{\eta}) = \min \left\{ 1, \frac{\pi(\zeta^* | \tilde{\zeta}, \tilde{\eta}) q(\tilde{\zeta} | \zeta^*, \tilde{\eta})}{\pi(\zeta^{(m)} | \tilde{\zeta}, \tilde{\eta}) q(\zeta^* | \tilde{\zeta}, \tilde{\eta})} \right\} = \min \left\{ 1, \frac{\pi(\zeta^* | \tilde{\eta}) q(\tilde{\zeta} | \zeta^*, \tilde{\eta})}{\pi(\zeta^{(m)} | \tilde{\eta}) q(\zeta^* | \tilde{\zeta}, \tilde{\eta})} \right\}, \quad (20)$$

where $\pi(\eta, \zeta)$ is the target distribution; otherwise, the current value is kept. The proposal distributions for Z_i^{HP} and $(\psi, Z_1^I, \dots, Z_n^I)$ are described in Sections 4.1 and 4.2 respectively. Naturally, the proposal distributions for θ depend on the choice of \mathcal{F}_H and $\mathcal{F}_{\text{prog}}$.

4.1 Metropolis-Hastings update for Z_i^{HP}

The efficiency of the Metropolis-Hastings steps for $Z_1^{HP}, \dots, Z_n^{HP}$ is central to the overall efficiency of our data-augmented Markov chain Monte Carlo sampler. We construct a proposal distribution for Z_i^{HP} that is independent of the

current value of this latent variable; a higher acceptance rate, therefore, results in better mixing. To this end, we design a proposal distribution that is close to the full conditional $\pi(Z_i^{HP} | \cdot)$. The support of $\pi(Z_i^{HP} | \cdot)$ is $(t_0, c_i] \cup \emptyset$ for individuals in the censored group and $(t_0, c_i]$ for those in the screen-detected and interval-detected groups. We therefore consider a proposal distribution with a positive density on the interval $(t_0, c_i]$ and a point mass at \emptyset for the censored group. The exact form of the proposal distribution depends on the group of the individual, described below.

4.1.1 Censored group

For an individual i in the censored group, the observed data consist of n_i negative screens and $t_i^{PC} = c_i$. The support of the full conditional distribution of Z_i^{HP} is $(t_0, c_i] \cup \emptyset$, and from Equations (9), (11) and (14), (15), its density is

$$\begin{aligned} \pi(Z_i^{HP} | \cdot) &\propto L_i(\theta, \psi; Z_i^{HP}, Z_i^I) f_t(t_i^{PC} | Z_i^{HP}, Z_i^I, \theta) f_O(O_1^i, \dots, O_{n_i}^i | Z_i^{HP}, \beta) \\ &\propto \left[\delta_{\emptyset}(Z_i^{HP}) S_{\mathsf{H}}(c_i - t_0) + \delta_{(t_0, c_i)}(Z_i^{HP}) f_{\mathsf{H}}(Z_i^{HP} - t_0; \theta) S_{\mathsf{prog}}(c_i - Z_i^{HP}; \theta)^{1-Z_i^I} \right] \beta^{m_i^+} (1 - \beta)^{m_i^-} (Z_i^{HP}) \\ &= \delta_{\emptyset}(Z_i^{HP}) S_{\mathsf{H}}(c_i - t_0) + \delta_{(t_0, c_i)}(Z_i^{HP}) f_{\mathsf{H}}(Z_i^{HP} - t_0; \theta) S_{\mathsf{prog}}(c_i - Z_i^{HP}; \theta)^{1-Z_i^I} (1 - \beta)^{m_i^-} (Z_i^{HP}). \end{aligned} \quad (21)$$

Here $m_i^+ = 0$ because person i belongs to the censored group, the notation $m_i^-(Z_i^{HP})$ emphasizes that the number of false negative screens is a function of Z_i^{HP} , and the equality holds because $m_i^-(\emptyset) = 0$. The full conditional (21) has a point mass at \emptyset and a positive density on $(t_0, c_i]$. The integer-valued quantity $m^-(Z_i^{HP})$ induces discontinuities, as shown in Figure 3a.

We construct a proposal distribution for the Metropolis-Hastings step that mimics the full conditional (21). First, the proposal has a point mass component at \emptyset with weight proportional to $S_{\mathsf{H}}(c_i - t_0)$. The density component is constructed as a mixture distribution with a discontinuous density proportional to $f_{\mathsf{H}}(Z_i^{HP} - t_0; \theta) (1 - \beta)^{m_i^-(Z_i^{HP})}$. The expression is designed to be equal to the full conditional distribution whenever the pre-clinical cancer is indolent ($Z_i^I = 1$), and otherwise only differs by the factor $S_{\mathsf{prog}}(c_i - Z_i^{HP}; \theta)$ for the case of progressive pre-clinical cancer. The mixture components are truncated Weibull distributions restricted to non-overlapping supports defined by the inter-screen intervals. Over the k th inter-screen interval $(t_{k-1}^i, t_k^i]$, the truncated Weibull density of the corresponding mixture component is proportional to $f_{\mathsf{H}}(Z_i^{HP} - t_0; \theta)$, and its mixture weight is proportional to

$$\int_{t_{j-1}^i}^{t_j^i} f_{\mathsf{H}}(Z_i^{HP} - t_0; \theta) (1 - \beta)^{n_i+1-k} dZ_i^{HP} = (1 - \beta)^{n_i+1-k} [F_{\mathsf{H}}(t_k^i - t_0; \theta) - F_{\mathsf{H}}(t_{k-1}^i - t_0; \theta)].$$

We choose to construct a mixture distribution whose continuous component has a density proportional to $f_{\mathsf{H}}(Z_i^{HP} - t_0; \theta) (1 - \beta)^{m_i^-(Z_i^{HP})}$ instead of $f_{\mathsf{H}}(Z_i^{HP} - t_0; \theta) S_{\mathsf{prog}}(c_i - Z_i^{HP}; \theta)^{1-Z_i^I} (1 - \beta)^{m_i^-(Z_i^{HP})}$ because the extra term $S_{\mathsf{prog}}(c_i - Z_i^{HP}; \theta)^{1-Z_i^I}$ makes the mixture components and weights intractable.

Putting everything together gives the mixed proposal distribution

$$q(Z_i^{HP} | \cdot) = p_0^i \delta_{\emptyset}(Z_i^{HP}) + \sum_{k=1}^{n_i+1} p_k^i \text{Trunc-}\mathsf{F}_{\mathsf{H}}(Z_i^{HP} - t_0; \theta, t_{k-1}^i - t_0, t_k^i - t_0) \quad (22)$$

where $\text{Trunc-}\mathsf{F}_{\mathsf{H}}(\cdot; \theta, l, u)$ is the distribution F_{H} truncated to the interval $(l, u]$, and where we set $t_0^i = t_0$ and $t_{n_i+1}^i = c_i$. The mixture weights are

$$p_0^i \propto S_{\mathsf{H}}(c_i - t_0), \quad (23)$$

$$p_k^i \propto (1 - \beta)^{n_i + 1 - k} [F_{\mathsf{H}}(t_k^i - t_0; \theta) - F_{\mathsf{H}}(t_{k-1}^i - t_0; \theta)], \quad k = 1, \dots, n_i + 1. \quad (24)$$

Here F_{H} is the cumulative distribution function of F_{H} . Because $p_k^i > 0, \forall k$, Equations (22)-(24) define a mixed distribution with a strictly positive density on its support $(t_0, c_i] \cup \emptyset$.

We sample from this distribution in a two-step procedure. First, we draw the index $k \in \{0, \dots, n_i + 1\}$ from the categorical distribution with weights p_0, \dots, p_{n_i+1} . The index $k = 0$ corresponds to the event that the P transition occurs after the censoring time, $k = 1$ that it occurs between t_0 and the first screen, the index $k = 2, \dots, n_i$ that it occurs between the $(k-1)$ th and the k th screen, and $k = n_i + 1$ that it occurs between the last screen and the censoring age. Second, we sample Z_i^{HP} conditionally on k as follows

$$Z_i^{HP} \mid k \sim \begin{cases} \delta_{\emptyset}(Z_i^{HP}), & k = 0 \\ \text{Trunc-}\mathsf{F}_{\mathsf{H}}(Z_i^{HP} - t_0; \theta, t_{k-1}^i - t_0, t_k^i - t_0), & k = 1, \dots, n_i + 1 \end{cases}, \quad (25)$$

This produces a proposal from (22), which is then accepted or rejected according to Equation (20) in the Metropolis-Hastings step.

4.1.2 Screen-detected cancer group

The observed data for individual i in the screen-detected group consist of negative screens followed by a positive screen at $t_{n_i}^i = c_i$. The support of the full conditional distribution of Z_i^{HP} is $(t_0, c_i]$, and its density is

$$\pi(Z_i^{HP} \mid \cdot) \propto f_{\mathsf{H}}(Z_i^{HP} - t_0; \theta) S_{\text{prog}}(c_i - Z_i^{HP}; \theta)^{1 - Z_i^{HP}} \beta^{m^+} (1 - \beta)^{m^-}(Z_i^{HP}), \quad (26)$$

where $\beta^{m^+} = \beta$ is a constant which we can drop by proportionality.

Following the same reasoning as in Section 4.1.1, we construct a proposal distribution consisting of a mixture of non-overlapping truncated Weibull distribution mimicking the full conditional (26). The proposal distribution is

$$q(Z_i^{HP} \mid \cdot) = \sum_{k=1}^{n_i} p_k^i \text{Trunc-}\mathsf{F}_{\mathsf{H}}(Z_i^{HP} - t_0; \theta, t_{k-1}^i - t_0, t_k^i - t_0), \quad (27)$$

where $t_0^i = t_0$, and the mixture weights are

$$p_k^i \propto (1 - \beta)^{n_i - k} [F_{\mathsf{H}}(t_k^i - t_0; \theta) - F_{\mathsf{H}}(t_{k-1}^i - t_0; \theta)], \quad k = 1, \dots, n_i. \quad (28)$$

Equations (27)-(28) define a mixture distribution with a positive density on $(t_0, c_i]$ from which we sample following the two-step procedure described in Section 4.1.1.

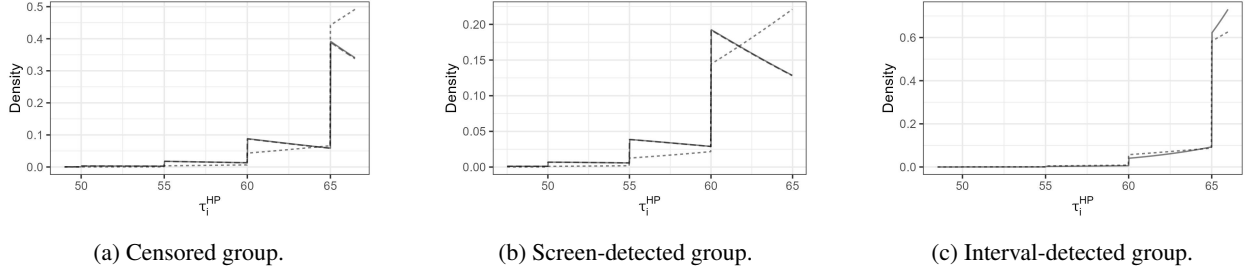


Figure 3: Comparison of the proposal and target densities in the Metropolis-Hastings step for the latent variable Z_i^{HP} . Solid line: proposal distribution $q(Z_i^{HP} | \cdot)$; dashed line: conditional distribution for progressive cancer $\pi(Z_i^{HP} | Z_i^I = 0, \cdot)$; long-dashed line: conditional distribution for indolent cancer $\pi(Z_i^{HP} | Z_i^I = 1, \cdot)$. In Panels (a) and (b), the proposal distribution matches exactly the conditional distribution for indolent cancers.

4.1.3 Interval cancer group

In the interval cancer group, the observed data for individual i consist of a series of negative screens followed by a clinical diagnosis at time $t_i^{PC} = \tau_i^{PC}$. Moreover, we have $Z_i^I = 0$ because the individual's pre-clinical cancer was necessarily progressive. The support of the full conditional distribution of Z_i^{HP} is $(t_0, c_i]$, and its density is

$$\pi(Z_i^{HP} | \cdot) \propto f_H(Z_i^{HP} - t_0; \theta) f_{\text{prog}}(c_i - Z_i^{HP}; \theta) (1 - \beta)^{m^-(Z_i^{HP})}. \quad (29)$$

As a proposal distribution, we employ the mixture distribution with density

$$q(Z_i^{HP} | \cdot) = \sum_{k=1}^{n_i+1} p_k^i \text{Trunc-F}_H(Z_i^{HP} - t_0; \theta, t_{k-1}^i - t_0, t_k^i - t_0), \quad (30)$$

where $t_0^i = t_0$ and $t_{n+1}^i = \tau_i^{PC}$, and the mixture weights are

$$p_k^i \propto (1 - \beta)^{n_i+1-k} [F_H(t_k^i - t_0) - F_H(t_{k-1}^i - t_0)], \quad k = 1, \dots, n_i + 1. \quad (31)$$

Equations (30)-(31) define a mixture distribution with a positive density on $(t_0, \tau_i^{PC}]$ from which we sample following the two-step procedure described in Section 4.1.1.

As illustrated in Figure 3, the three proposal distributions (22), (27) and (30) all closely match their corresponding full conditional distributions, resulting in a high acceptance rate in the Metropolis-Hastings steps (see also the simulations and case study in Sections 5-6). In the case of a progressive pre-clinical cancer, the proposal distribution—which ignores the term S —is close to the full conditional distribution, and in the case of an indolent pre-clinical cancer, the proposal distribution matches exactly the full conditional distribution (see Figures 3a-3b). Moreover, the proposals do not depend on Z_i^I , a fact which will be useful in Section 4.4.

4.2 Joint Metropolis-Hastings update for $(\psi, Z_1^I, \dots, Z_n^I)$

We update ψ and the vector (Z_1^I, \dots, Z_n^I) jointly because these two objects are highly correlated a posteriori due to the observed data providing little information about the latent indolent status of censored and screen-detected individuals.

At iteration $m = 1, \dots, M$ of the sampler, we use the two-step proposal distribution

$$q\left(\psi^*, Z_1^I, \dots, Z_n^I \mid \psi^{(m)}, \cdot\right) = q_\psi\left(\psi^* \mid \psi^{(m)}\right) q_I\left(\left(Z_1^I, \dots, Z_n^I\right)^* \mid \psi^*, \cdot\right), \quad (32)$$

which first samples a new value ψ^* and then samples a new vector $(Z_1^I, \dots, Z_n^I)^*$ conditionally on ψ^* .

The proposal distribution $q_\psi\left(\psi^* \mid \psi^{(m)}\right)$ corresponds to a Gaussian random walk with reflection at 0 and 1, ensuring that $\psi^* \in [0, 1]$. Simple algebra shows that the proposal distribution q_ψ is symmetric, and its variance ϵ is a tuning parameter. If ϵ is too small, the Markov chain will take small steps, inefficiently exploring the space of ψ , while if ϵ is too large, most proposed values will be rejected, resulting in a Markov chain that is often stuck at the same location. In our implementation of the sampler, we tune the value of ϵ to reach a pre-specified acceptance rate during an warmup phase using the adaptive procedure described in [Hoffman et al., 2014], and then fix ϵ for the remaining iterations. Details of the adaptive procedure are provided in Appendix E.

Next, $(Z_1^I, \dots, Z_n^I)^*$ is sampled conditionally on ψ^* by drawing each Z_i^I independently from its full conditional distribution given ψ^* . If a person i is diagnosed with an interval cancer, we set $Z_i^I = 0$ as their cancer is necessarily progressive; otherwise

$$\pi(Z_i^I \mid \psi^*, \cdot) = \text{Ber}(q_i), \quad (33)$$

where

$$q_i = \Pr\left(Z_i^I = 1 \mid \psi^*, \cdot\right) = \frac{L_i\left(Z_i^I = 1; \psi^*, \cdot\right)}{L_i\left(Z_i^I = 0; \psi^*, \cdot\right) + L_i\left(Z_i^I = 1; \psi^*, \cdot\right)}, \quad (34)$$

with

$$L_i(Z_i^I; \psi^*, \cdot) = \begin{cases} \text{Ber}(Z_i^I; \psi^*), & Z_i^{HP} = \emptyset, \\ \text{Ber}(Z_i^I; \psi^*) S_{\text{prog}}\left(c_i - Z_i^{HP}; \theta\right)^{1-Z_i^I}, & Z_i^{HP} \leq c_i \end{cases}, \quad (35)$$

the likelihood of Z_i^I .

4.3 Metropolis-Hastings update for θ

We update the elements of θ in separate univariate Metropolis-Hastings steps using a Gaussian random walk proposal. Further complete details of these steps are described in Appendix B.

4.4 Initialization of the sampler

To initialize the sampling algorithm, one only needs to specify the initial values of (θ, ψ, β) . Given some initial values $(\theta^{(0)}, \psi^{(0)}, \beta^{(0)})$, we generate the initial values of the latent variables using the proposal distributions of the Metropolis-Hastings steps. Specifically, the initial values $Z_1^{HP(0)}, \dots, Z_n^{HP(0)}$ are generated independently using the distributions (22), (27) and (30) based on the group—censored, screen-detected cancer or interval cancer—of each individual, and $(Z_1^I, \dots, Z_n^I)^{(0)}$ are generated from (33) independently.

4.5 Theoretical guarantees

Theorem 2 shows that the Markov chain underlying the data-augmented Markov chain Monte Carlo sampler is ergodic. The ergodic theorem, therefore, holds for any π -integrable function h , and the estimator $\bar{h}_m = \frac{1}{m} \sum_{i=1}^m h(\theta^{(i)}, \beta^{(i)}, \mathbf{Z}^{(i)})$ is asymptotically consistent for $E_\pi h$ under any initial distribution [Billingsley, 2017].

Theorem 2 (Ergodicity). *The Markov chain $\{(\theta^{(m)}, \theta^{(m)}, z^{(m)})\}_{m=1}^M$ underlying the data-augmented Markov chain Monte Algorithm algorithm described in this article is ergodic.*

Proof. We follow the proof of Morsomme and Xu [2022]. By construction, the distribution $\pi(\theta, \psi, \beta, \mathbf{Z} \mid \mathbf{Y})$ is invariant for the kernels $P_\beta, P_\theta, P_{Z_i^{HP}}$ (for $i = 1, \dots, n$) and P_{ψ, Z^I} that respectively update β, θ, Z_i^{HP} and $(\psi, Z_1^I, \dots, Z_n^I)$. The distribution $\pi(\theta, \psi, \beta, \mathbf{Z} \mid \mathbf{Y})$ is, therefore, also invariant for the composite kernel $P = P_\beta P_\theta P_{Z_1^{HP}} \dots P_{Z_n^{HP}} P_{\psi, Z^I}$ [Tierney, 1994]. Moreover, as each kernel is strictly positive, P is also strictly positive. As a result, the chain is π -irreducible and aperiodic. The chain is, therefore, positive Harris recurrent and thus ergodic. \square

4.6 Model comparison

Mis-specifying a model of cancer natural history can lead to biased inference [Cheung et al., 2022]. To identify specifications for F_H and F_{prog} that fit the data well, we compare the predictive fit of models with different choices for these distributions. We accomplish this by extending approximate leave-one-out cross-validation (ALOOCV) Gelfand et al. [1992], Gelfand [1995], Vehtari et al. [2017] to the class of latent variable models. While exact cross-validation requires fitting the model multiple times, approximate cross-validation can be easily computed from the posterior draws of a MCMC sampler. The procedure is straight-forward to implement, and enables a hypothesis test for the difference in predictive fit between models.

We define the leave-one-out out-of-sample predictive fit as

$$\text{pf} = \sum_{i=1}^n \log(f(y_i \mid \mathbf{Y}_{-i})), \quad (36)$$

where $\mathbf{Y}_{-i} = (Y_1, \dots, Y_{i-1}, Y_{i+1}, \dots, Y_n)$ denotes the data set without the i th subject and

$$f(y_i \mid \mathbf{Y}_{-i}) = \int f(y_i \mid \theta, \psi, \beta) \pi(\theta, \psi, \beta \mid \mathbf{Y}_{-i}) d\theta d\psi d\beta, \quad (37)$$

is the predictive density for subject i given the data of the other subjects, and prefer model with larger predictive fit.

We approximate Eq (37) using the importance sampling estimator

$$\hat{f}(y_i \mid \mathbf{Y}_{-i}) = \frac{\sum_{m=1}^M r_i^{(m)} f(y_i \mid \theta^{(m)}, \psi^{(m)}, \beta^{(m)})}{\sum_{m=1}^M r_i^{(m)}}, \quad (38)$$

with importance weight $r_i^{(m)} = \frac{\pi(\theta, \psi, \beta \mid \mathbf{Y}_{-i})}{g(\theta^{(m)}, \psi^{(m)}, \beta^{(m)})}$ for some proposal distribution g .

Vehtari et al. [2017] suggest to choose

$$g(\theta, \psi, \beta) = \pi(\theta, \psi, \beta \mid \mathbf{Y}) \quad (39)$$

for two reasons. First, for large samples $\pi(\theta, \psi, \beta \mid \mathbf{Y})$ tends to be similar to $\pi(\theta, \psi, \beta \mid \mathbf{Y}_{-i})$, making it a suitable proposal distribution for importance sampling. Second, by construction, once the Markov chain has reached stationarity the draws $\{(\theta^{(m)}, \psi^{(m)}, \beta^{(m)})\}_m$ come from $\pi(\theta, \psi, \beta \mid \mathbf{Y})$, making the proposal (39) straightforward to implement. This choice of proposal results in the importance weight

$$\begin{aligned} r_i^{(m)} &= \frac{\pi(\theta^{(m)}, \psi^{(m)}, \beta^{(m)} \mid \mathbf{Y}_{-i})}{\pi(\theta^{(m)}, \psi^{(m)}, \beta^{(m)} \mid \mathbf{Y})} \\ &\propto \frac{f(\mathbf{Y}_{-i} \mid \theta^{(m)}, \psi^{(m)}, \beta^{(m)})}{f(\mathbf{Y} \mid \theta^{(m)}, \psi^{(m)}, \beta^{(m)})} \\ &= \frac{1}{f(y_i \mid \theta^{(m)}, \psi^{(m)}, \beta^{(m)})}, \end{aligned}$$

giving the estimator

$$\hat{f}(y_i \mid \mathbf{Y}_{-i}) = \left(\frac{1}{M} \sum_{m=1}^M \frac{1}{f(y_i \mid \theta^{(m)}, \psi^{(m)}, \beta^{(m)})} \right)^{-1}, \quad (40)$$

where $\{(\theta^{(1)}, \psi^{(1)}, \beta^{(1)}) \dots, (\theta^{(M)}, \psi^{(M)}, \beta^{(M)})\}$ correspond to the posterior draws of the MCMC sampler. Finally, we estimate the out-of-sample predictive fit (36) with

$$\hat{\text{pf}} = \sum_{i=1}^n \log(\hat{f}(y_i \mid \mathbf{Y}_{-i})) = - \sum_{i=1}^n \log \left(\frac{1}{M} \sum_{m=1}^M \frac{1}{f(y_i \mid \theta^{(m)}, \psi^{(m)}, \beta^{(m)})} \right). \quad (41)$$

4.6.1 Estimating $f(y_i \mid \theta, \psi, \beta)$

For our model, the likelihood $f(y_i \mid \theta, \psi, \beta)$ does not admit a closed-form expression. We use importance sampling to estimate this quantity, taking advantage of the expression

$$\begin{aligned} f(y_i \mid \theta, \psi, \beta) &= \int f(y_i, Z_i \mid \theta, \psi, \beta) dZ_i \\ &= \int f(y_i \mid \theta, \psi, \beta, Z_i) f(Z_i \mid \theta, \psi, \beta) dZ_i. \end{aligned} \quad (42)$$

Equation (42) suggests the importance sampling estimate

$$\hat{f}(y_i \mid \theta, \psi, \beta) = \frac{1}{J} \sum_{j=1}^J f(y_i \mid \theta, \psi, \beta, Z_i^j) w^j,$$

with importance weights $w^j = \frac{f(Z_i^j \mid \theta, \psi, \beta)}{q(Z_i^j)}$ for some proposal distribution q .

We choose q to correspond to the Metropolis-Hastings proposal distributions for the latent variables described in Section 4.1-4.2,

$$q(Z_i) = q_{\text{HP}}(Z_i^{HP} \mid \cdot) q_l(Z_i^l \mid Z_i^{HP}, \cdot), \quad (43)$$

with q_{HP} corresponding to Equation 22, 27 or 30 based on the group of individual i , and q_l corresponding to Equation 33. We sample $Z_i \sim q$ sequentially, first sampling $Z_i^{HP} \sim q_{HP}$ and then sampling $Z_i^I \mid Z_i^{HP} \sim q_l$.

Substituting $\hat{f}(y_i \mid \theta, \psi, \beta)$ for $f(y_i \mid \theta, \psi, \beta)$ in (41) gives the predictive fit estimate

$$\hat{pf} = \sum_{i=1}^n \log(\hat{f}(y_i \mid \mathbf{Y}_{-i})) = - \sum_{i=1}^n \log \left(\frac{1}{M} \sum_{m=1}^M \frac{1}{\frac{1}{J} \sum_{j=1}^J f(y_i \mid \theta^{(m)}, \psi^{(m)}, \beta^{(m)}, Z_i^{(j)}) w^j} \right). \quad (44)$$

Appendix C describes a t -test of the hypothesis that two models have the same predictive fit (36).

4.7 Model implementation

The methodology described in Section 3.3 applies to any continuous distribution F_H and F_{prog} on the positive line. For the simulations in Section 5 and the case study in Section 6, we choose $F_H = \text{Wei}(\lambda_H, \alpha_H)$ and $F_{\text{prog}} = \text{Wei}(\lambda_{\text{prog}}, \alpha_{\text{prog}})$, with $\text{Wei}(\lambda, \alpha)$ denoting the Weibull distribution with rate $\lambda > 0$ and shape $\alpha > 0$, and whose density is proportional to $x^{\alpha-1} \exp\{-\lambda x^\alpha\}$. The Weibull choice has several advantages, including flexibility and interpretability: if $\alpha > 1$ ($\alpha < 1$), the hazard function increases (decreases) with age as $\propto t^{\alpha-1}$; and if $\alpha = 1$ it corresponds to the exponential distribution. In addition, the Weibull distribution's survival function has a closed-form expression, and its cumulative distribution function can be inverted, which enables efficient sampling from Trunc- F_H in (22), (27) and (30).

We implement the MCMC sampler in the programming language C++ for efficiency. The sampler is fast, scaling to cohort studies with tens of thousands of individuals. For convenience, the C++ implementation is made available in R via the R package `baclava` with the help the package RCPP [Eddelbuettel and François, 2011]. In the MCMC runs in Sections 5-6, we keep 10^3 thinned draws post warm-up phase due to memory constraints.

5 Performance on simulated data

To examine the mixing properties of our sampler, we run multiple MCMC samplers initialized at over-dispersed values on a simulated dataset. We then use the potential scale reduction factor [Gelman and Rubin, 1992, Brooks and Gelman, 1998], the effective sample size and traceplots to assess the algorithm's mixing properties.

For the purposes of a synthetic dataset, we set the starting age for non-zero onset hazard to $t_0 = 30$ years, and assume a linear increase in both the onset and progression hazards ($\alpha_H = \alpha_{\text{prog}} = 2$). We further set the Weibull rates to $\lambda_H = 6.5 \times 10^{-5}$ and $\lambda_{\text{prog}} = 3.14 \times 10^{-2}$, resulting in a cumulative risk of pre-clinical onset by age 80 of 15%, and a mean sojourn time of $\mu_{\text{prog}} = 5$ years. Finally, we set the indolent probability to $\psi = 0.1$ and the screen sensitivity to $\beta = 0.85$. We simulate the natural histories of cancer among $n = 40,000$ individuals (see Appendix D for the distributions of screening and censoring ages).

We employ the independent prior distributions $\pi(\lambda_H, \lambda_{\text{prog}}, \psi, \beta) = \pi(\lambda_H)\pi(\lambda_{\text{prog}})\pi(\psi)\pi(\beta)$ with

$$\pi(\lambda_H) = \text{Ga}(1, 0.01), \quad \pi(\lambda_{\text{prog}}) = \text{Ga}(1, 0.01), \quad \pi(\psi) = \text{Be}(1, 1), \quad \pi(\beta) = \text{Be}(38.5, 5.8)$$

Parameter	Potential scale reduction factor	Effective sample size
λ_H	1.0005	11,728
λ_{prog}	1.0027	2,731
ψ	1.002	2,568
β	1.0013	6,497

Table 1: Performance of the MCMC sampler on simulated data.

We choose these prior distributions for their flexibility and, in the case of $\pi(\beta)$, for its conjugacy (Theorem 1). The prior distribution on λ_H , λ_{prog} and ψ are weakly informative, and that of β places 95% of its mass on the interval (0.76, 0.95), reflecting prior empirical data on the performance of mammography screening of clinicians about that parameter [Lehman et al., 2017].

Next, we apply our MCMC sampler to the synthetic dataset and estimate the values of the parameters λ_H , λ_{prog} , ψ and β . We independently run 20 MCMC samplers initialized at over-dispersed values of these parameters (the latent variables need not be initialized, see Section 4.4). The initial values $\lambda_H^{(0,m)}$, $\lambda_{\text{prog}}^{(0,m)}$, $\psi^{(0,m)}$ and $\beta^{(0,m)}$ of the m th sampler ($m = 1, \dots, 20$) are sampled from a wide interval around the true values, mutually independently,

$$\lambda_H^{(0,m)} \sim \text{Unif}(2 \times 10^{-5}, 2 \times 10^{-4}), \quad \lambda_{\text{prog}}^{(0,m)} \sim \text{Unif}(10^{-2}, 10^{-1}), \quad \psi^{(0,m)} \sim \text{Unif}(0, 1), \quad \beta^{(0,m)} \sim \text{Unif}(0.7, 0.95).$$

For each chain, we set the warm-up period to 10^4 iterations and run the sampler for an additional 2×10^4 iterations. Table 1 shows that the potential scale reduction factor, computed on the post warm-up thinned draws with the R package `coda` [Plummer et al., 2006], is smaller than 1.005 for all parameters, indicating that the chains—which were initialized at over-dispersed values—converged during the warmup phase and mixed adequately once they reached stationarity [Gelman and Rubin, 1992]. This is a remarkable achievement considering the high dimensional latent space with 80,000 latent variables.

In addition to exploring the parameter space efficiently, the sampler also explores the space of the latent variables swiftly. Figure 4 displays the MCMC draws of the latent variables for an individual whose cancer was screen-detected at age 58 years, after a series of five consecutive negative screens. The individual had 5 negative screens at ages . The traceplots of the indolent indicator (Figure 4a) and the pre-clinical transition time (Figure 4b) indicate that the sampler rapidly explores the latent space. In particular, the frequent switches between the values 0 and 1 of the binary draws in Figure 4a show that the Markov chain is not stuck in any particular configuration of the latent variables for any large number of iterations.

An interesting feature of our data augmentation approach is that we obtain a patient-specific estimate of the onset time of pre-clinical cancer, a quantity that is unobservable in practice. Figure 4c illustrates the MCMC approximation of the marginal posterior distribution $\pi(\tau^{HP} | \mathbf{Y})$ for the above individual with a screen-detected cancer at age 58 years. Because the screening sensitivity is high, it is most likely that the time of onset took place after the last screen at 55 years, less likely that it did between the screens at ages 53 and 55, and extremely unlikely before the screen at age

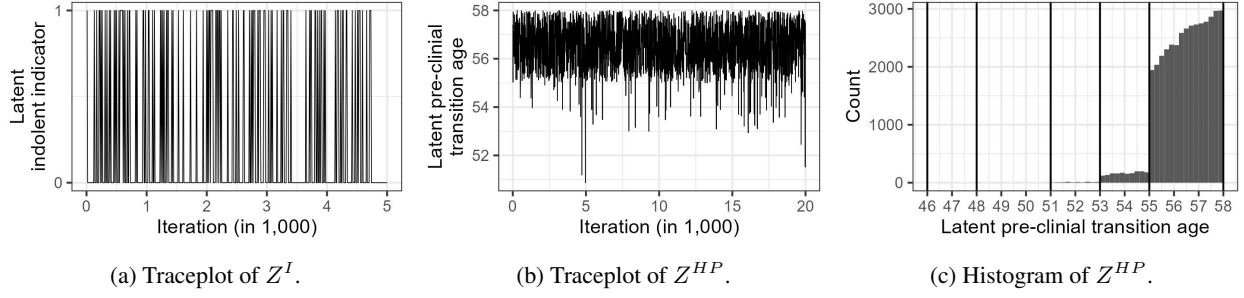


Figure 4: Markov chain Monte Carlo draws from the first chain ($m = 1$) for the latent variables of an individual with a screen-detected cancer at age 58 and five negative screens at ages (46, 48, 51, 53, 55). Panel (a) is a traceplot of the latent indolent indicator over an interval of 5,000 iterations for clarity. Panel (b) is a traceplot of the latent pre-clinical transition age. Panel (c) shows the marginal posterior distribution of the latent pre-clinical transition age; vertical lines depict the ages at which the screens occur.

53. As illustrated by the discontinuities in this histogram, the screens themselves contribute most of the information available about the unobserved onset age of pre-clinical cancer.

6 Application to data from the Breast Cancer Surveillance Consortium

We illustrate the utility of our semi-Markov model and accompanying data-augmented MCMC sampler with an analysis of the screening and cancer diagnosis histories from participants in the Breast Cancer Surveillance Consortium (BCSC), a large population-based mammography screening registry in the US [Ballard-Barbash et al., 1997]. The BCSC registries collect mammography results and link them to breast outcomes and vital status through linkage with regional population-based SEER (Surveillance, Epidemiology, and End Results) programs, state tumor registries, and state death records.

We used the analytic cohort previously described in Ryser et al. [2022], including $n = 35,986$ women aged 50 to 74 years who received their first screening mammogram at a BCSC facility between 2000 and 2018 (Table 2). Each BCSC registry and the Statistical Coordinating Center (SCC) have received institutional review board approval for all study procedures, including passive permission (one registry), a waiver of consent (six registries), or both depending on facility (one registry), to enroll participants, link data, and perform analytic studies. All procedures are Health Insurance Portability and Accountability Act (HIPAA) compliant. All registries and the SCC have received a Federal Certificate of Confidentiality and other protections for the identities of women, physicians, and facilities who are subjects of this research.

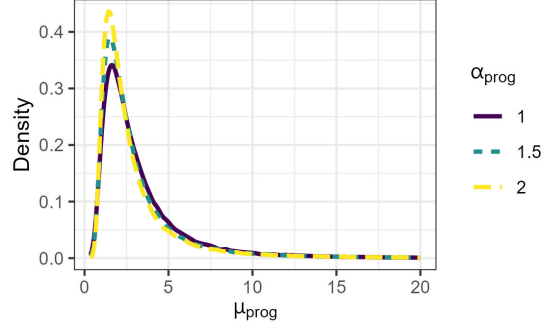
Following Ryser et al. [2022], we set $t_0 = 30$. We employ the independent prior distributions $\pi(\lambda_H, \lambda_{\text{prog}}, \psi, \beta) = \pi(\lambda_H)\pi(\lambda_{\text{prog}})\pi(\psi)\pi(\beta)$ with

$$\pi(\lambda_H) = \text{Ga}(1, 0.01), \quad \pi(\lambda_{\text{prog}}) = \text{Ga}(a_{\text{prog}}, b_{\text{prog}}), \quad \pi(\psi) = \text{Be}(1, 1), \quad \pi(\beta) = \text{Be}(38.5, 5.8),$$

Characteristic	Value
Median (IQR) age at first screen, years	56 (52-64)
Median (IQR) number screens	1 (1-3)
Median (IQR) inter-screen interval, years	1.39 (1.05-2.19)
Number of interval-detected cancers	73
Number of screen-detected cancers	645
Number of censored individuals	35,268

Table 2: Summary of the data from the Breast Cancer Surveillance Consortium (n=35,986). IQR: Inter-quartile range.

α_{prog}	a_{prog}	b_{prog}
1	2.64	5.75
1.5	1.36	4.28
2	0.9	3.56



(a) Parameters of $\text{Ga}(a_{\text{prog}}, b_{\text{prog}})$.

(b) Implied prior distribution of μ_{prog} .

Figure 5: Weakly informative prior distribution of λ_{prog} .

where, for a given α_{prog} , we choose values for a_p and b_p that induce a weakly informative distribution on the mean sojourn time μ_{prog} with 0.9 mass in the interval (1, 9) years, reflecting prior knowledge about breast cancer progression (Figure 5a) . Figure 5b shows that the prior distributions induced on μ_{prog} are similar across values of α_{prog} .

6.1 Model specification

We consider the 21 models with $\alpha_H \in \{1, 1.5, 2, 2.5, 3, 4, 5\}$ and $\alpha_{\text{prog}} \in \{1, 1.5, 2\}$. We fit each model to the BCSC data and compare them via ALOOCV (see Section 4.6). The warm-up period is set to 2×10^4 iterations and is followed by an additional 5×10^4 iterations, resulting in an effective sample size of at least 10^3 for each parameter in every setting.

Figure 6 displays the predictive fit of the models. The relation between predictive fit and α_H follows an inverted-U shape, and, nominally, the best model fit was achieved at $\alpha_H = 4$ and $\alpha_{\text{prog}} = 1$. Models with $\alpha_H \leq 1.5$ and 2 of the 3 models with $\alpha_H = 2$ have an estimated predictive fit that is significantly different from that of the best model at the significance level 0.05. This shows that letting the pre-clinical hazard rate increase at least linearly with age significantly improves the predictive fit of the model for the BCSC data set. However, the exact speed of the increase—linear, quadratic, etc—cannot be inferred from the data, probably because the available screens only cover the range 50-85 years, with 97% of them limited to the range 50-75 years.

In contrast, α_{prog} does not have significant impact on the predictive fit. The three lines in Figure 6, which correspond to the three values of this parameter, are extremely close to one another, and the pairwise differences between the

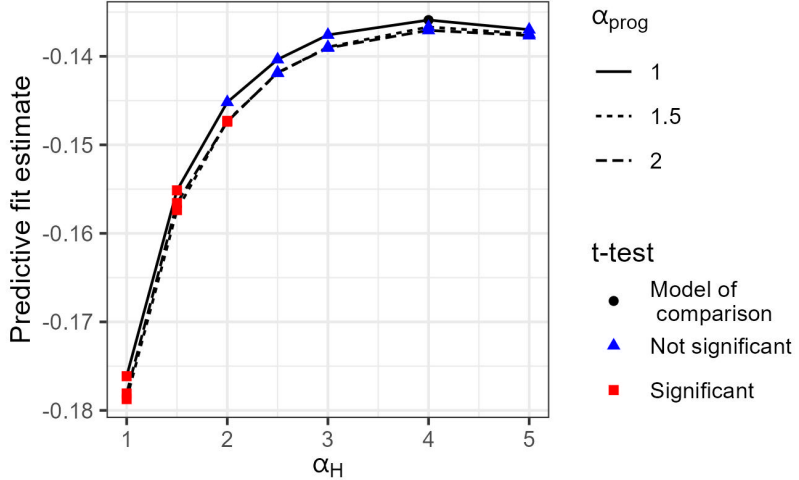


Figure 6: Predictive fit of the models on the BCSC data. The black dot denotes the best model. The red squares correspond to models whose predictive score is significantly different from that of the best model, based on a two-sample t-test at the significance level 0.05). The blue triangle correspond to models whose predictive fit is not significantly different from that of the best model.

predictive fit of models with the same α_H did not reach statistical significance at $\alpha = 0.05$. This indicates that the data contain little information about this parameter. This is to be expected because the endpoints of the pre-clinical sojourn times of progressive cancer are mostly unobserved. Indeed, the start age is never exactly observed; furthermore, as the screens are imperfect, this value is not even interval censored. In addition, the end age of the sojourn is exactly observed only for the interval-detected group (0.18% of the sample) and is right-censored for the other individuals.

This observation drives us to motivate the choice biologically. In particular, we choose a value of α_{prog} that implies realistic predictive distributions of sojourn times among progressive cancers. Conditional on λ_{prog} , the sojourn time of a progressive cancer—denoted by σ_{prog} —follows the Weibull distribution $\text{Wei}(\lambda_{\text{prog}}, \alpha_{\text{prog}})$. Its predictive distribution

$$\pi(\sigma_{\text{prog}} | \mathbf{Y}, \alpha_{\text{prog}}) = \int \text{Wei}(\sigma_{\text{prog}}; \lambda_{\text{prog}}, \alpha_{\text{prog}}) \pi(\lambda_{\text{prog}} | \mathbf{Y}, \alpha_{\text{prog}}) d\lambda_{\text{prog}}, \quad (45)$$

is therefore a rate-mixture of Weibull distributions, in which the Weibull rate is integrated out. We approximate the posterior distribution $\pi(\lambda_{\text{prog}} | \mathbf{Y}, \alpha_{\text{prog}})$ with the empirical distribution of the MCMC draws $\{\lambda_{\text{prog}}^{(1)}, \dots, \lambda_{\text{prog}}^{(M)}\}$, giving the Rao-Blackwell estimate of the predictive distribution (45) [Robert et al., 2007]

$$\hat{\pi}(\sigma_{\text{prog}} | \mathbf{Y}, \alpha_{\text{prog}}) = \frac{1}{M} \sum_{m=1}^M \text{Wei}\left(\sigma_{\text{prog}}; \lambda_{\text{prog}}^{(m)}, \alpha_{\text{prog}}\right). \quad (46)$$

Figure 7a presents the estimate (46) for the three models with $\alpha_H = 2.5$ and $\alpha_{\text{prog}} \in \{1, 1.5, 2\}$. Under $\alpha_{\text{prog}} = 1$, the predictive distribution has a large amount of mass concentrated at 0 and a thick tail to the right. In contrast, under the semi-Markov model with $\alpha_{\text{prog}} \in \{1.5, 2\}$ the density of the predictive distribution has a thin tail to the right, and no mass concentrated at 0. Figure 7b presents the probabilities that the sojourn time of a future individual is less than 0.5 year and more than 15 years for the different values of α_{prog} . Under $\alpha_{\text{prog}} = 1$, these probabilities amount to

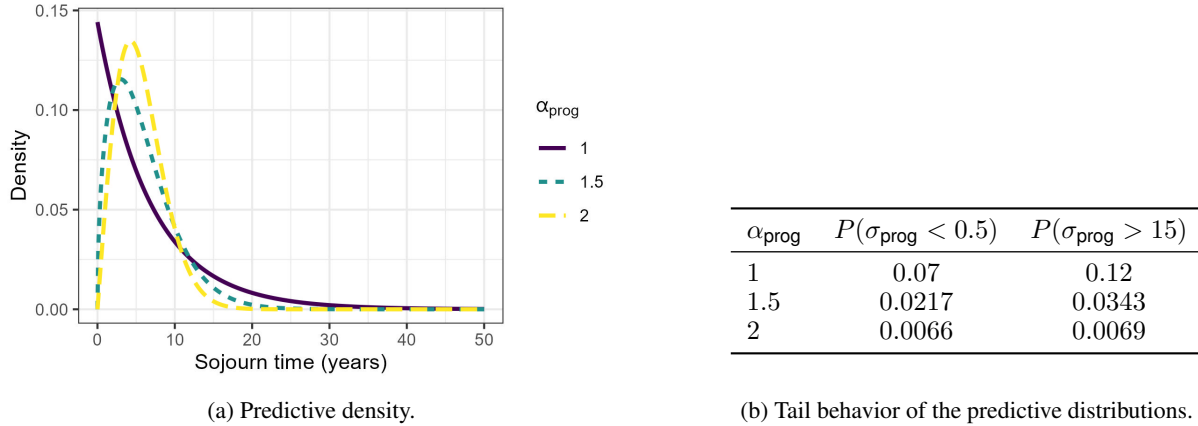


Figure 7: Predictive distribution of pre-clinical sojourn times among progressive cancers for the Breast Cancer Surveillance Consortium dataset ($\alpha_H = 2.5$).

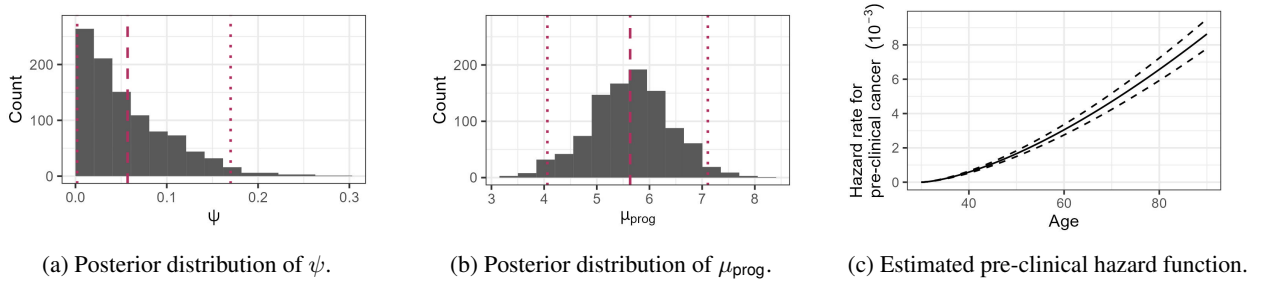


Figure 8: Results of the analysis of the data set from the Breast Cancer Surveillance Consortium data set. Panels (a) and (b) display the marginal posterior distributions of the fraction of indolent pre-clinical cancers (ψ) and the mean sojourn time among progressive pre-clinical cancers (μ_{prog}), respectively. The posterior means (dashed red line) and 95% credible intervals (dotted red lines) are included. Panel (c) shows the estimated pre-clinical hazard rate as a function of age, with the posterior median (solid line) and 95% credible band (dashed lines) indicated.

almost 20% of progressive cancers with an extremely short or long pre-clinical sojourn time, while for the models with $\alpha_{\text{prog}} = 1.5, 2$, they amount to 5.6% and 1.3% respectively. We thus opt for $\alpha_{\text{prog}} = 2$ because it results in a more realistic model of sojourn times and note that the user can use any other value for this parameter deemed suitable.

Among the models with $\alpha_{\text{prog}} = 2$, we choose the one with $\alpha_H = 2.5$ because it agrees with the trend in age-specific data from the Surveillance, Epidemiology, and End Results Program and its predictive fit is not significantly different from that of the best model. Figure 8 presents the output of the MCMC sampler for the chosen model. The posterior mean of the indolence probability ψ is 0.057, with 95% credible interval (0.002 – 0.17), and that of the mean sojourn time of a progressive cancer μ_{prog} is 5.63 years (95% CI: 4.06 – 7.11). Finally, the hazard rate for pre-clinical cancer at age 40 is estimated to be 0.59×10^{-3} (95% CI: 0.53×10^{-3} – 0.65×10^{-3}) and that at age 80 is estimated to be 6.6×10^{-3} (95% CI: 5.9×10^{-3} – 7.2×10^{-3}), and the probability of pre-clinical onset by age 80 is estimated to be 12.3% (95% CI: 11.2% – 13.4%), similar to the usual estimate of lifetime incidence of breast cancer of 1/8.

α_H	α_{prog}	Overdiagnosis rate	Source		Mean sojourn time	Probability of Indolence (%)
			Mortality from Indolence	Mortality from other causes		
2.5	1	15.6 (5.4, 28.9)	5.3 (0.1, 19.2)	10.3 (2.8, 22)	7.1 (5.3, 9.1)	4.2 (0.1, 14.9)
2.5	1.5	13 (3.8, 25.7)	5.7 (0.1, 19)	7.3 (1.6, 17.5)	5.9 (4.5, 7.6)	4.7 (0.1, 15.5)
2.5	2	13.4 (3.6, 26.9)	6.9 (0.2, 22.3)	6.6 (1.4, 15.9)	5.6 (4.1, 7.1)	5.7 (0.2, 17)
Ryser et al. [2022]		15.4 (9.4, 26.5)	6.1 (0.2, 20.1)	9.3 (5.5, 13.5)	6.6 (4.9, 8.6)	4.5 (0.1, 14.8)

Table 3: Estimates of the overdiagnosis rate and the respective contribution of indolence and mortality from other causes for the three models with $\alpha_H = 2.5$ and the model of Ryser et al. [2022]. The posterior means and 95% credible intervals are reported.

6.2 Estimation of the overdiagnosis rate

Using our MCMC draws, we can estimate the posterior of any function of the parameters. Here, we focus on the extent of *overdiagnosis* in a screening program, defined as the the mammographic detection of cancer that would not become clinically evident in the woman’s remaining lifetime. There are two contributions to overdiagnosis. First, by definition, every non-progressive cancer that is detected on mammography is overdiagnosed. Second, progressive screen-detected cancer are overdiagnosed if the time from screen-detection to death from a breast cancer-unrelated cause is shorter than the time from screen-detection to clinical progression (also referred to as the lead-time). We use the breast cancer natural history estimates from the BCSC cohort to estimate the overdiagnosis rate in a biennial screening program from age 50 to 74 years. Table 3 provides a side-by-side comparison of the three models with $\alpha_H = 2.5$. The three models yield similar estimate for the overdiagnosis rate and the respective contribution indolence and mortality from other sources, showing that these results are robust to the choice of α_{prog} . This is reassuring given that the ALOOCV procedure was unable to delineate the best value of this parameter. Moreover, the estimates we obtain are in line with those of Ryser et al. [2022], which are based on a Markov model with a piece-wise constant onset rate for pre-clinical cancer, corroborating the claim that approximately 1 in 7 screen-detected breast cancers are overdiagnosed.

7 Discussion

In this paper, we introduce an efficient data-augmented MCMC sampling algorithm for fitting a flexible family of semi-Markov mixture models of cancer natural history to individual-level screening and cancer diagnosis histories. By allowing for age-dependent pre-clinical onset hazards, non-exponentially distributed sojourn times, and a mixture of indolent and progressive tumors, we substantially expand the range of cancer progression models and dynamics amenable to rigorous Bayesian inference via MCMC. These advances are a marked departure from prior approaches, which relied on simple Markov models for tractability. Our sampler efficiently explores the high-dimensional joint space of model parameters and latent variables, and automatically quantifies individual-level uncertainty of clinically relevant quantities such as a person’s pre-clinical onset time, indolence status, and sojourn time.

A key application of our methodology is the estimation of screening-related overdiagnosis rates. In the motivating example of breast cancer, overdiagnosis has been documented as the chief harm of screening, yet there is substantial residual uncertainty about its true extent. Due to the counterfactual nature of overdiagnosis, its estimation is methodologically challenging and, as in our case of observational data from a screened cohort, relies on sound estimates of the latent tumor progression dynamics. Applying our method to a high-quality cohort of women undergoing mammography screening, we make two important observations. First, our breast cancer overdiagnosis estimates are similar to those previously derived from the same cohort using a slightly different model structure, thus adding weight to the finding that approximately 1 in 7 screen-detected breast cancers are overdiagnosed. Second, although the data contain insufficient information to delineate the best-fitting sojourn time parameterization, we find that the overdiagnosis estimates were robust to changes in this parameterization. This finding of robustness is particularly important because model misspecification is guaranteed when modeling complex biological processes such as cancer progression. Finally, we note that thanks to the latent data augmentation, our approach provides individual-level estimates of the time of onset with pre-clinical cancer. These data could, for example, be leveraged to derive individual level estimation of overdiagnosis.

Future efforts will be directed toward methodological extensions of our approach, including covariate-dependent hazard rates, non-parametric formulations of the pre-clinical onset hazard for additional flexibility, and the introduction of early and late disease stages. In the meantime, the current iteration of the method, as available through the R package `baclava`, has the potential to facilitate rigorous natural history estimation across various cancers with available screening data.

Acknowledgements. This research was funded by the National Cancer Institute (R35-CA274442) and the National Science Foundation (DMS 2230074 and PIPP 2200047). Data collection for this research was funded by the National Cancer Institute (P01CA154292, U01CA63736, U01CA069976). The collection of cancer and vital status data was supported in part by several state public health departments and cancer registries (<https://www.bscs-research.org/work/acknowledgement>). We thank the participating women, mammography facilities, and radiologists for the data they have provided. You can learn more about the BCSC at: <http://www.bscs-research.org/>. All statements in this report, including its findings and conclusions, are solely those of the authors and do not necessarily represent the views of the National Cancer Institute or the National Institutes of Health.

References

H Gilbert Welch and William C Black. Overdiagnosis in cancer. *Journal of the National Cancer Institute*, 102(9): 605–613, 2010.

Stephen W Duffy and Dharmishta Parmar. Overdiagnosis in breast cancer screening: the importance of length of observation period and lead time. *Breast Cancer Research*, 15:1–9, 2013.

Nicholas E Day and Stephen D Walter. Simplified models of screening for chronic disease: estimation procedures from mass screening programmes. *Biometrics*, pages 1–13, 1984.

Yu Shen and Marvin Zelen. Parametric estimation procedures for screening programmes: stable and nonstable disease models for multimodality case finding. *Biometrika*, 86(3):503–515, 1999.

Carolyn M Rutter and James E Savarino. An evidence-based microsimulation model for colorectal cancer: validation and application. *Cancer epidemiology, biomarkers & prevention*, 19(8):1992–2002, 2010.

Arnaud Seigneurin, Olivier François, José Labarère, Pierre Oudeville, Jean Monlong, and Marc Colonna. Overdiagnosis from non-progressive cancer detected by screening mammography: stochastic simulation study with calibration to population based registry data. *Bmj*, 343, 2011.

Anne Helene Olsen, Olorunsola F Agbaje, Jonathan P Myles, Elsebeth Lynge, and Stephen W Duffy. Overdiagnosis, sojourn time, and sensitivity in the copenhagen mammography screening program. *The Breast Journal*, 12(4):338–342, 2006.

Wendy Yi-Ying Wu, Sven Törnberg, Klara Miriam Elfström, Xijia Liu, Lennarth Nyström, and Håkan Jonsson. Overdiagnosis in the population-based organized breast cancer screening program estimated by a non-homogeneous multi-state model: a cohort study using individual data with long-term follow-up. *Breast Cancer Research*, 20(1):1–11, 2018.

Stephen W Duffy, Olorunsola Agbaje, Laszlo Tabar, Bedrich Vitak, Nils Bjurstam, Lena Björneld, Jonathan P Myles, and Jane Warwick. Overdiagnosis and overtreatment of breast cancer: estimates of overdiagnosis from two trials of mammographic screening for breast cancer. *Breast Cancer Research*, 7:1–8, 2005.

Marc D Ryser, Jane Lange, Lurdes YT Inoue, Ellen S O'Meara, Charlotte Gard, Diana L Miglioretti, Jean-Luc Bulliard, Andrew F Brouwer, E Shelley Hwang, and Ruth B Etzioni. Estimation of breast cancer overdiagnosis in a us breast screening cohort. *Annals of internal medicine*, 175(4):471–478, 2022.

Carolyn M Rutter, Diana L Miglioretti, and James E Savarino. Bayesian calibration of microsimulation models. *Journal of the American Statistical Association*, 104(488):1338–1350, 2009.

Oguzhan Alagoz, Mehmet Ali Ergun, Mucahit Cevik, Brian L Sprague, Dennis G Fryback, Ronald E Gangnon, John M Hampton, Natasha K Stout, and Amy Trentham-Dietz. The university of wisconsin breast cancer epidemiology simulation model: an update. *Medical decision making*, 38(1_suppl):99S–111S, 2018.

Laura Bondi, Marco Bonetti, Denitsa Grigorova, and Antonio Russo. Approximate bayesian computation for the natural history of breast cancer, with application to data from a milan cohort study. *Statistics in Medicine*, 2023.

Dirk F Moore, Nilanjan Chatterjee, David Pee, and Mitchell H Gail. Pseudo-likelihood estimates of the cumulative risk of an autosomal dominant disease from a kin-cohort study. *Genetic epidemiology: the official publication of the international genetic epidemiology society*, 20(2):210–227, 2001.

Hsin-Ju Hsieh, Tony Hsiao-Hsi Chen, and Shu-Hui Chang. Assessing chronic disease progression using non-homogeneous exponential regression markov models: an illustration using a selective breast cancer screening in taiwan. *Statistics in medicine*, 21(22):3369–3382, 2002.

Li C Cheung, Paul S Albert, Shruti Kona Das, and Richard J Cook. Multistate models for the natural history of cancer progression. *British Journal of Cancer*, 127(7):1279–1288, 2022.

Martin A Tanner and Wing Hung Wong. The calculation of posterior distributions by data augmentation. *Journal of the American statistical Association*, 82(398):528–540, 1987.

Mark Girolami and Ben Calderhead. Riemann manifold langevin and hamiltonian monte carlo methods. *Journal of the royal statistical society series B: statistical methodology*, 73(2):123–214, 2011.

Alan E Gelfand, Dipak K Dey, and Hong Chang. Model determination using predictive distributions with implementation via sampling-based methods. *Bayesian statistics*, 4:147–167, 1992.

Alan E Gelfand. Model determination using sampling-based methods. *Markov chain Monte Carlo in practice*, page 145, 1995.

Aki Vehtari, Andrew Gelman, and Jonah Gabry. Practical bayesian model evaluation using leave-one-out cross-validation and waic. *Statistics and computing*, 27:1413–1432, 2017.

Marc D Ryser, Roman Gulati, Marisa C Eisenberg, Yu Shen, E Shelley Hwang, and Ruth B Etzioni. Identification of the fraction of indolent tumors and associated overdiagnosis in breast cancer screening trials. *American journal of epidemiology*, 188(1):197–205, 2019.

Yu Shen and Marvin Zelen. Screening sensitivity and sojourn time from breast cancer early detection clinical trials: mammograms and physical examinations. *Journal of Clinical Oncology*, 19(15):3490–3499, 2001.

Stuart G Baker, Philip C Prorok, and Barnett S Kramer. Lead time and overdiagnosis, 2014.

Hsiu-Hsi Chen, Stephen W Duffy, and Laszlo Tabar. A markov chain method to estimate the tumour progression rate from preclinical to clinical phase, sensitivity and positive predictive value for mammography in breast cancer screening. *Journal of the Royal Statistical Society Series D: The Statistician*, 45(3):307–317, 1996.

Joseph Berkson and Robert P Gage. Survival curve for cancer patients following treatment. *Journal of the American Statistical Association*, 47(259):501–515, 1952.

Yingwei Peng and Jeremy MG Taylor. Cure models. *Handbook of survival analysis*, 34:113–134, 2014.

Andrew Gelman, John B Carlin, Hal S Stern, David B Dunson, Aki Vehtari, and Donald B Rubin. *Bayesian data analysis*. CRC press, 2013.

Steve Brooks, Andrew Gelman, Galin Jones, and Xiao-Li Meng. *Handbook of markov chain monte carlo*. CRC press, 2011.

Matthew D Hoffman, Andrew Gelman, et al. The no-u-turn sampler: adaptively setting path lengths in hamiltonian monte carlo. *J. Mach. Learn. Res.*, 15(1):1593–1623, 2014.

Patrick Billingsley. *Probability and measure*. John Wiley & Sons, 2017.

Raphael Morsomme and Jason Xu. Exact inference for stochastic epidemic models via uniformly ergodic block sampling. *arXiv preprint arXiv:2201.09722*, 2022.

Luke Tierney. Markov chains for exploring posterior distributions. *The annals of statistics*, pages 1701–1728, 1994.

Dirk Eddelbuettel and Romain François. Rcpp: Seamless r and c++ integration. *Journal of statistical software*, 40:1–18, 2011.

Andrew Gelman and Donald B Rubin. Inference from iterative simulation using multiple sequences. *Statistical science*, 7(4):457–472, 1992.

Stephen P Brooks and Andrew Gelman. General methods for monitoring convergence of iterative simulations. *Journal of computational and graphical statistics*, 7(4):434–455, 1998.

Constance D. Lehman, Robert F. Arao, Brian L. Sprague, Janie M. Lee, Diana S. M. Buist, Karla Kerlikowske, Louise M. Henderson, Tracy Onega, Anna N. A. Tosteson, Garth H. Rauscher, and Diana L. Miglioretti. National performance benchmarks for modern screening digital mammography: Update from the breast cancer surveillance consortium. *Radiology*, 283(1):49–58, 2017.

Martyn Plummer, Nicky Best, Kate Cowles, Karen Vines, et al. Coda: convergence diagnosis and output analysis for mcmc. *R news*, 6(1):7–11, 2006.

Rachel Ballard-Barbash, Stephen H Taplin, Bonnie C Yankaskas, Virginia L Ernster, Robert D Rosenberg, Patricia A Carney, William E Barlow, Berta M Geller, Karla Kerlikowske, Brenda K Edwards, et al. Breast cancer surveillance consortium: a national mammography screening and outcomes database. *AJR. American journal of roentgenology*, 169(4):1001–1008, 1997.

Christian P Robert et al. *The Bayesian choice: from decision-theoretic foundations to computational implementation*, volume 2. Springer, 2007.

Herbert Robbins and Sutton Monro. A stochastic approximation method. *The annals of mathematical statistics*, pages 400–407, 1951.

Andrew Gelman, Gareth O Roberts, and Walter R Gilks. Efficient metropolis jumping rules. *Bayesian statistics 5*, 5: 599–608, 1996.

Christophe Andrieu and Johannes Thoms. A tutorial on adaptive mcmc. *Statistics and computing*, 18:343–373, 2008.

A Proof of Theorem 1

Proof. From Equations (9), (13) and (18), the joint distribution of $(\theta, \psi, \beta, \mathbf{Z}, \mathbf{Y})$ is

$$\begin{aligned}\pi(\theta, \psi, \beta, \mathbf{Z}, \mathbf{Y}) &= \pi(\theta, \psi, \beta) f(\mathbf{Y} \mid \theta, \psi, \beta, \mathbf{Z}) L(\theta, \psi; \mathbf{Z}) \\ &= \pi(\beta) \pi(\theta, \psi) \beta^{m^+} (1 - \beta)^{m^-} \prod_{i=1}^n f_t(t_i^{PC} \mid Z_i, \theta) L(\theta, \psi; \mathbf{Z}),\end{aligned}\quad (47)$$

From Equation (47), the full conditional distribution of β is, by proportionality,

$$\begin{aligned}\pi(\beta \mid \theta, \psi, \mathbf{Z}, \mathbf{Y}) &\propto \pi(\theta, \psi, \beta, \mathbf{Z}, \mathbf{Y}) \\ &\propto \pi(\beta) \beta^{m^+} (1 - \beta)^{m^-} \\ &\propto \beta^{a+m^+-1} (1 - \beta)^{b+m^--1},\end{aligned}$$

which is the kernel of the distribution $\text{Be}(a + m^+, b + m^-)$.

□

B Metropolis-Hastings updates for the Weibull rate parameters of \mathbf{F}_H and \mathbf{F}_{prog}

The proposal distributions in the Metropolis-Hastings steps for λ_H and λ_{prog} correspond to normal random walks on the positive line with a reflection at 0. At step $m = 1, \dots, M$, the candidate values are

$$\lambda_H^* \mid \lambda_H^{(m-1)} = |\lambda_H^{(m-1)} + \eta_H|, \quad \eta_H \sim N(0, \epsilon_H), \quad (48)$$

and

$$\lambda_{\text{prog}}^* \mid \lambda_{\text{prog}}^{(m-1)} = |\lambda_{\text{prog}}^{(m-1)} + \eta_{\text{prog}}|, \quad \eta_{\text{prog}} \sim N(0, \epsilon_{\text{prog}}), \quad (49)$$

where ϵ_H and ϵ_P are tuning parameters and the absolute values ensure that the proposed values are positive.

Simple algebra shows that the proposal distributions (48) and (49) are symmetrical. For λ_H , the Metropolis-Hastings acceptance probability (20), therefore, simplifies to

$$\alpha(\lambda_H^{m-1} \rightarrow \lambda_H^*) = \min \left\{ 1, \frac{\pi(\theta^*, \psi, \beta, \mathbf{Z} \mid \mathbf{Y})}{\pi(\theta^{(m-1)}, \psi, \beta, \mathbf{Z} \mid \mathbf{Y})} \right\} = \min \left\{ 1, \frac{\pi(\theta^*) L(\theta^*, \psi; \mathbf{Z})}{\pi(\theta^{(m-1)}) L(\theta^{(m-1)}, \psi; \mathbf{Z})} \right\},$$

where $\theta^* = (\lambda_H^*, \lambda_{\text{prog}}, \psi)$ contains the proposed value for λ_H , and $\theta^{(m-1)} = (\lambda_H^{(m-1)}, \lambda_{\text{prog}}, \psi)$ the current value. The second equality holds by Equations (9)-(17). The acceptance probability for λ_{prog} is analogous. We use adaptive Markov chain Monte Carlo to find values of ϵ_H and ϵ_{prog} that yield a pre-specified acceptance rate; details are provided in Appendix E.

C Hypothesis test for approximate leave-one out cross-validation

Given two models A and B , the model with the largest predictive fit (36) is better. Consider the difference between the estimates of the two models

$$\Delta_{AB} = \widehat{\text{pf}}_A - \widehat{\text{pf}}_B = \sum_{i=1}^n \Delta_{AB}^i,$$

where $\Delta_{AB}^i = \log(\widehat{f}_A(y_i | \mathbf{Y}_{-i})) - \log(\widehat{f}_B(y_i | \mathbf{Y}_{-i}))$ is the difference between the contributions of individual i . We now describe a paired t-test for the null hypothesis that $\Delta_{AB} = 0$. To estimate the standard error of Δ_{AB} , we take advantage of the fact that the data of the same subjects are used to compute $\widehat{\text{pf}}_A$ and $\widehat{\text{pf}}_B$ and use the paired estimate

$$SE(\Delta_{AB}) = \sqrt{n \text{Var}_{i=1}^n(\Delta_{AB}^i)}, \quad (50)$$

where $\text{Var}_{i=1}^n a_i = \frac{1}{n-1} \sum_{i=1}^n (a_i - \bar{a})^2$.

We can then appeal to the Central Limit Theorem to describe the asymptotic behavior of Δ_{AB} . By exchangeability of the subjects, Δ_{AB} is a sum of identically distributed random variables with finite variance. These random variable are, however, not entirely independent; the source of dependence between Δ_{AB}^i and Δ_{AB}^j comes from conditioning on the data of subject j when evaluating Δ_{AB}^i and conditioning on the data of subject i from j when evaluating Δ_{AB}^j . For large n , however, the influence of a single subject becomes negligible, resulting in quasi independence between Δ_{AB}^i and Δ_{AB}^j . The conditions for a paired t -test are, therefore, satisfied in large samples, with the t -statistic

$$t = \frac{\Delta_{AB}}{SE(\Delta_{AB})}, \quad (51)$$

and $n - 1$ degrees of freedom.

D Details of the simulated data in Section 5

The age of the first screen is sampled from the categorical distribution with weights $w_k \propto \exp\{-k/5\}$ for $k = 40, 41, \dots, 80$. Inter-screen intervals are sampled from the distribution $\text{Poisson}(0.5)$ plus 1 year, resulting in a mean inter-screen interval of 1.5 years. Finally, for individual $i = 1, \dots, n$, the age of last follow-up is $\min\{100, t_1^i + W_i\}$ with $W_i \sim \text{Exp}(1/5)$ independently over i , implying that individuals remain in the screening program for 5 years on average.

E Adaptive Markov chain Monte Carlo

The Metropolis-Hastings steps for $(\psi, Z_1^I, \dots, Z_n^I)$, λ_H and λ_{prog} rely on normal random walk proposals governed by a step size parameter. We use the adaptive procedure of Hoffman et al. [2014] for finding values for the step size parameters that result in a pre-specified acceptance rate. We now describe this procedure.

Consider the generic case of a random walk Metropolis-Hastings step where the normally distributed increments have variance $\epsilon > 0$. ϵ acts as a step size parameter, and we wish to find a value $\bar{\epsilon}$ such that the acceptance rate reaches some desired value $\delta \in (0, 1)$.

Write $H_m = \delta - \alpha_m$, where $\alpha_m \in [0, 1]$ is the Metropolis-Hastings acceptance probability at step $m = 1, \dots, M$. We apply the update

$$\log(\epsilon_{m+1}) = (1 - \omega_t) \log(\epsilon_t) + \omega_m \xi_{m+1}, \quad (52)$$

where

$$\xi_{m+1} = -\frac{\sqrt{m}}{\gamma} \frac{1}{m + m_0} \sum_{i=1}^m H_i, \quad (53)$$

is the correction term at step $m + 1$ and $\omega_m = m^{-\kappa}$.

This iterative procedure is a stochastic approximation method. Formula (52), introduced by Hoffman et al. [2014], gives more weight to later iterations than the classical update of Robbins and Monro [1951]. This is desirable in the setting of MCMC as early iterations correspond to the transient phase of the Markov chain which may be quite different from its recurrent phase. Formula (52), therefore, ensures that the early iterations do not have a disproportionate weight in the tuning procedure.

In the Metropolis-Hastings step for $(\psi, Z_1^I, \dots, Z_n^I)$, we set the desired acceptance rate to 0.24 as it is a high-dimensional update, while in the steps for λ_H and λ_{prog} we set it to 0.44 as they are univariate updates [Gelman et al., 1996]. Following Hoffman et al. [2014], we further set $\gamma = 0.05$, $m_0 = 10$, and $\kappa = 0.75$, which is sufficient to ensure that $\sum_{m=1}^{\infty} \omega_m = \infty$ and $\sum_{m=1}^{\infty} \omega_m^2 < \infty$, as is required for ϵ_m to converge to $\bar{\epsilon}$ [Andrieu and Thoms, 2008].

Given a total number of iteration M and a number of warm up iterations $W < M$, we use the iterations $m = 1, \dots, W$ as a warm up phase during which the step size ϵ is tuned using Formula (52). We then use the value ϵ_W found at the end of the warm-up phase for the remaining iterations. The warm-up iterations are discarded when we estimate the posterior distribution.